

© 2016 IEEE. Personal use of this material is permitted. Permission from IEEE must be obtained for all other uses, in any current or future media, including reprinting/republishing this material for advertising or promotional purposes, creating new collective works, for resale or redistribution to servers or lists, or reuse of any copyrighted component of this work in other works.

Digital Object Identifier (DOI): 10.1109/TSG.2016.2614846

IEEE Transactions on Smart Grid (Volume:PP, Issue:99) October 2016

Load Control using Sensitivity Identification by means of Smart Transformer

Giovanni De Carne
Giampaolo Buticchi
Marco Liserre
Costas Vournas

Suggested Citation

G. De Carne; G. Buticchi; M. Liserre; C. Vournas, "Load Control using Sensitivity Identification by means of Smart Transformer," in *IEEE Transactions on Smart Grid*, vol.PP, no.99, pp.1-1

Load Control using Sensitivity Identification by means of Smart Transformer

Giovanni De Carne, *Student Member, IEEE*, Giampaolo Buticchi, *Member, IEEE*, Marco Liserre, *Fellow, IEEE*, and Costas Vournas, *Fellow, IEEE*

Abstract—The higher variability introduced by distributed generation leads to fast changes in the aggregate load composition, and thus in the power response during voltage variations. The Smart Transformer, a power electronics-based distribution transformer with advanced control functionalities, can exploit the load dependence on voltage for providing services to the distribution and transmission grids. In this paper two possible applications are proposed: the Smart Transformer overload control by means of voltage control action, and the Soft Load Reduction method, that reduces load consumption avoiding the load disconnection. These services depend on the correct identification of load dependence on voltage, which the Smart Transformer evaluates in real time based on load measurements. The effect of the distributed generation on net load sensitivity has been derived and demonstrated with the Control Hardware In Loop evaluation by means of a Real Time Digital Simulator.

Index Terms—Smart Transformer, Solid State Transformer, load voltage sensitivity, load reduction, overload control.

I. INTRODUCTION

THE penetration of Distributed Generation (DG), mostly based on renewable energy sources (RES), has increased the demand variability in the power grid [1]. The DG variability can impact adversely the control actions on the grid. For instance, voltage control for stability purposes [2][3], or voltage and frequency regulation [4][5], without a proper understanding of the aggregate load active and reactive power response to voltage variations, may lead to an incorrect estimate of grid stability [6]. Particular attention in the last years has been given to the Conservation Voltage Reduction (CVR) method, where energy saving can be achieved by decreasing the voltage in the grid [7][8]. However, in all the above cases the load sensitivities to voltage variation are assumed known *a priori* and are not evaluated in real time. Thus a proper identification of load sensitivity with respect to voltage is of vital importance for correct control actions.

The load dependence on voltage has been object of study in the literature for many years [9][10][11]. Identifying the load active and reactive power response to voltage and frequency variations, however, presents several challenges. Even when the behavior of the single load is well known in the lab, or

The research leading to these results has received funding from the European Research Council under the European Union's Seventh Framework Programme (FP/2007-2013) / ERC Grant Agreement n. [616344] - HEART.

Giovanni De Carne, Giampaolo Buticchi, Marco Liserre are with the Chair of Power Electronics, University of Kiel, Kiel, Germany, e-mail: gdc@tf.uni-kiel.de

Costas Vournas is with the School of Electrical and Computer Engineering, National Technical University, Athens, Greece, email: vournas@power.ece.ntua.gr

in simulation, the aggregate load sensitivity to voltage is difficult to be evaluated. Two approaches have been adopted for identifying the aggregate load characteristic: the component-based method, and the measurement-based method [6], [12]-[13]. The first approach implies experimental tests of load components and then aggregating them in composite loads [14]. In the second approach the measurements are taken from the field and the parameters of the loads are estimated by fitting methods [15]. The latter approach is largely employed by utilities due to the availability of field measurements [16]. The aforementioned methods require a long data history and are computationally demanding. This represents a limitation for on-line control actions due to the high variability of DG, and load composition.

The Smart Transformer (ST) is a power electronic transformer [17]. It enables the control of voltage amplitude and frequency of low voltage (LV) grid independently from the medium voltage (MV) grid (Fig. 1). The ST can offer additional services to the LV grid, such as voltage balancing in presence of unbalanced loads, and interaction with the local loads and generators to avoid overload conditions [18][19]. When the On-Line Load Identification method [20] is implemented in a ST, the load active and reactive power response to voltage and frequency variation can be evaluated in real time, and subsequent corrective control actions can take into account the actual load response.

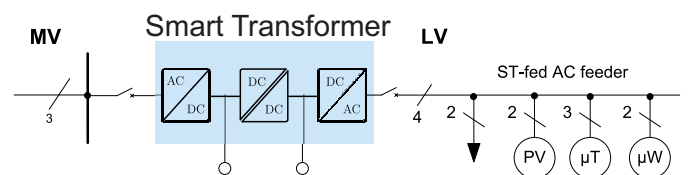


Fig. 1. Three-stages Smart Transformer in a LV AC distribution grid.

This paper introduces the mathematical and experimental verification of on-line load sensitivity identification including the effect of DG on the evaluated voltage sensitivities. It is demonstrated how, in the presence of DG, the aggregate load dependence on voltage increases with respect to the passive load case. The On-Line Load Identification method is used in the paper for two services: the Soft Load Reduction following a request by the system operator, and the Voltage-Based Overload Control of the ST. The first application is an alternative to the firm load shedding method. It reduces the consumed power by means of voltage variation without disconnecting the load in the LV grid. In the second application, the correct

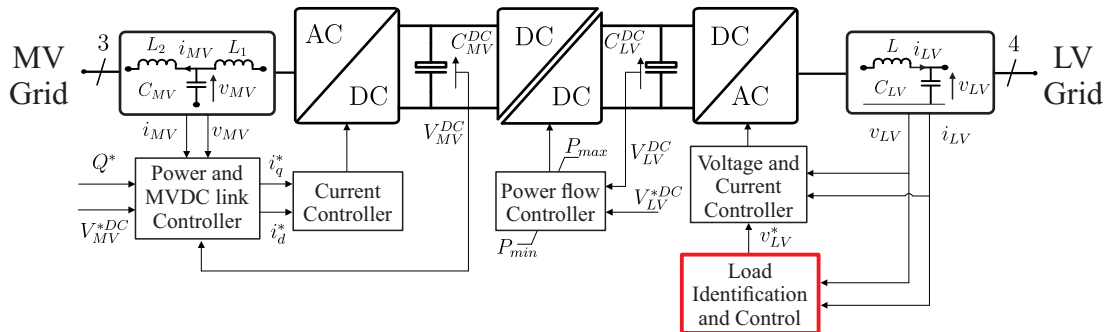


Fig. 2. Smart Transformer control scheme.

identification of voltage load sensitivity allows calculating the appropriate voltage variation to alleviate the overload of the ST. If the load is constant impedance, a voltage decrease leads to current decrease [18]; on the contrary, with constant power load the voltage decrease worsens the ST overload, increasing the current.

The paper is structured as follows: in Section II the ST concept and control is described; the operation principle of the On-Line Load Identification method and the influence of DG in the sensitivity measurement are described in Section III. The services offered by the Load Identification and Control are introduced in Section IV. Their experimental verification is performed with the Control-Hardware-In-Loop (CHIL) concept by means of a Real Time Digital Simulator (RTDS) in Section V. In Section VI the accuracy analysis of the On-Line Load Identification and the experimental verification of the effect of DG on the voltage sensitivity measurement are discussed. Finally Section VII draws the conclusions.

II. THE SMART TRANSFORMER CONCEPT

The Smart Transformer is a three-stage power electronics transformer [17][21] that adapts the voltage between the MV to the LV grid and provides new services to the distribution grid. Although several topology solutions can be studied for each stage [22], the control strategies do not differ substantially. In fact there is no indication for a preferred topology due to the fact that the ST must adapt itself to the grid to which it is connected (grounding, voltage level, number of phases). The LV side provides symmetrical voltage waveforms in the LV grid. The amplitude and shape of the current waveform is determined solely by the load. The DC/DC converter performs two tasks: (i) transforms the voltage from MV to LV and (ii) controls the voltage value of the LV DC link, thus keeping the balance between input and output active power. The MV side keeps the MV DC link voltage fixed to the nominal value, exchanging the needed power in the MV grid. The control strategy of the ST is shown in Fig. I.

In addition to controlling the voltage in the MV DC link, the MV converter controls also the reactive power injection in the MV grid. In ordinary conditions, the ST works with constant power factor, setting the reactive power reference to zero. In case ancillary services are requested from the ST (for instance voltage support in the MV grid), the ST can provide reactive power. The reactive power set-point can be evaluated locally

by means of a V/Q droop controller curve, or set remotely from a centralized controller.

The DC/DC regulates the power flow between the two DC stages keeping the LV DC link voltage constant to the nominal value. The reference power is limited between the P_{max} , determined by the ST rating, and P_{min} . The value of P_{min} can be set equal to $-P_{max}$ (allowing bi-directional flow), or equal to zero, if a limitation of reverse power flow is desired. In this case, the interaction with the local generation, for example by means of frequency variation [23], is necessary.

The LV converter is controlled by means of a voltage and a current control loops, in order to keep the voltage waveform sinusoidal with constant amplitude and frequency under any load condition. In this application the voltage waveform reference is given by the On-Line Load Identification controller (Fig. I, red box), explained in the next section.

III. ON-LINE LOAD IDENTIFICATION

A. Load Sensitivity Measurement

The basic idea of the On-Line Load Identification method is to apply a ramp variation of the chosen variable (voltage or frequency) by means of the ST, and measure the active and reactive power consumption during the ramp, in order to compute the voltage and frequency load sensitivity coefficients. In this paper only the voltage dependence of active and reactive power of load has been considered.

The load sensitivity to voltage is normalized as follows

$$\begin{aligned} K_p &= \frac{\Delta P/P_0}{\Delta V/V_0} \\ K_Q &= \frac{\Delta Q/Q_0}{\Delta V/V_0} \end{aligned} \quad (1)$$

where P_0 , Q_0 , V_0 are respectively the values of the active and reactive powers and *RMS* voltages at the ST busbar at the time the measurement is taken; ΔP and ΔQ the active and reactive power variations following the voltage disturbance ΔV . If the exponential model is used, i.e. if it is assumed that:

$$\begin{aligned} P &= P_0 (V/V_0)^{K_p} \\ Q &= Q_0 (V/V_0)^{K_q} \end{aligned} \quad (2)$$

then the load voltage sensitivities K_p and K_q defined in (3) are equal to the corresponding exponents of (2) [24].

In order to evaluate the voltage sensitivity coefficients of the grid load, the control logic in Fig.3 is applied. The On-Line Load Identification controller (Fig.I, red box) applies a trapezoidal voltage disturbance as described in [20]. At specified time instants during the voltage variation the ST measures the line currents and phase-to-ground voltages. Then the single-phase active and reactive powers P and Q are evaluated and stored in memory together with the *RMS* voltage V . Using the measured values at time t_k and the previous time instant t_{k-1} , the sensitivities at time t_k are computed as in [20]:

$$K_p = \frac{\frac{P(t_k) - P(t_{k-1})}{P(t_{k-1})}}{\frac{V(t_k) - V(t_{k-1})}{V(t_{k-1})}} \quad (3)$$

$$K_q = \frac{\frac{Q(t_k) - Q(t_{k-1})}{Q(t_{k-1})}}{\frac{V(t_k) - V(t_{k-1})}{V(t_{k-1})}}$$

and stored in memory.

This sequence is repeated in the following time instant until the end of the voltage ramp. The final value of the sensitivities is obtained averaging all the values stored during the time window considered.

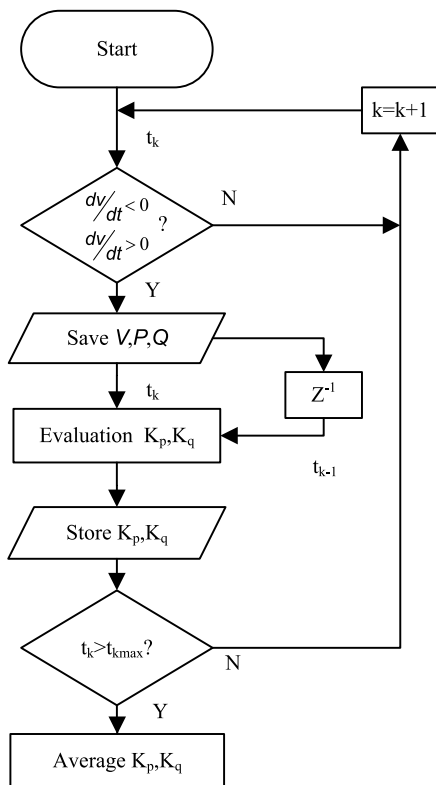


Fig. 3. Flow chart of the Voltage On-Line Load Identification method

B. Effect of DG in voltage sensitivity values

When a significant DG penetration is present, a marked effect on the sensitivity of the net feeder load is expected. This section is focused on the active power sensitivities, assuming that the DG is operating at unity power factor so that $Q_G = 0$.

Assuming a feeder with connected load P_L and distributed generation $P_G < P_L$ (i.e. the feeder is still providing power) the net load seen by the feeder is:

$$P_0 = P_L - P_G > 0 \quad (4)$$

if the load P_L has a normalized voltage sensitivity $K_{p,L}$:

$$K_{p,L} = \frac{\Delta P_L / P_L}{\Delta V / V_0} \quad (5)$$

and the active power of the DG is insensitive to voltage (considering negligible its contribution to the losses), i.e. $K_{p,G} = 0$, the net feeder load changes for a voltage disturbance ΔV as follows:

$$\Delta P = \Delta P_L = K_{p,L} (\Delta V / V_0) P_L \quad (6)$$

Using (3), (5) and (6) the apparent feeder load sensitivity is given by:

$$K_p = \frac{\Delta P / P_0}{\Delta V / V_0} = K_{p,L} \frac{P_L}{P_L - P_G} \quad (7)$$

The net load sensitivity is used in order to estimate the effectiveness of voltage reduction in controlling feeder load (as will be discussed in the next section) and it depends on the (unknown a priori) DG penetration. Clearly (7) is meaningless when the DG penetration is close or exceeds 100%. If the DG is participating in voltage regulation, a more detailed analysis is necessary to model the coordination between feeder and DG voltage control and to incorporate the effect of Q_G in overall load behavior.

IV. LOAD IDENTIFICATION APPLICATIONS

The On-line Load Identification and Control is represented with more details in Fig.4. At each time step, the controller measures current and voltage from the ST filter and performs a first security check on the power, voltage and current limits. If the ST receives the request of load reduction, it triggers the Soft Load Reduction control. If the security current limit of ST is exceeded (here fixed at 95% of the maximum current), ST limit controller overrides any control action and triggers the Voltage-Based Overload Control (see Section IV.B).

A. Soft Load Reduction control

Load shedding is an extreme measure to be adopted when the stability of the grid can be compromised due to severe contingencies: faults, generators disconnections, lines tripping [25]. However, firm load shedding is a harmful measure for the disconnected customers and incurs considerable costs. [26]. The ST can decrease the consumed load active power by controlling the voltage in the LV grid in accordance with load sensitivity, thus realizing a softer load reduction. The accuracy of this method depends on the knowledge of the load active power dependence on voltage. In order to guarantee to the Transmission (TSO) and Distribution System Operator (DSO) a pre-specified load reduction, an accurate analysis of the load sensitivity is needed. The On-Line Load Identification can perform this analysis and provide accurate data on load composition, and thus an accurate load reduction when needed.

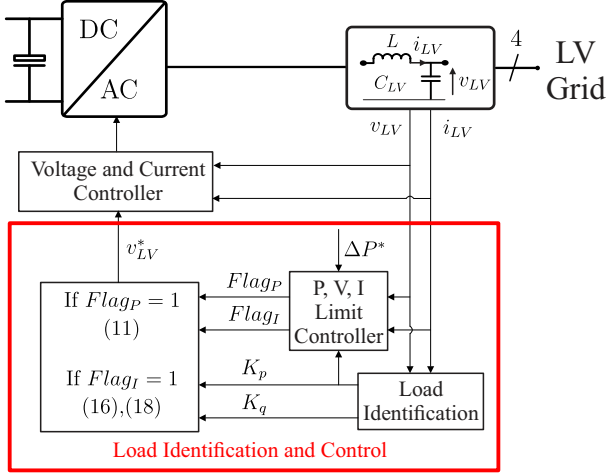


Fig. 4. Load Identification and Control scheme

In an unbalanced three-phase system it is possible that each phase has a different load sensitivity. Thus the proposed algorithm evaluates separately the sensitivities K_P and K_Q of each phase, using a simultaneous balanced three-phase load disturbance. Assuming a required percentage of load reduction $0 < \gamma < 1$, the desired load change will be:

$$\Delta P = \Delta P_A + \Delta P_B + \Delta P_C = -\gamma(P_A + P_B + P_C) \quad (8)$$

where P_A, P_B, P_C are the initial consumed active powers in each phase and $\Delta P_A, \Delta P_B, \Delta P_C, \Delta P$ the corresponding phase and total load variations.

Applying (3) to all three phases:

$$\begin{aligned} \Delta P_A &= \frac{P_A}{V_A} K_{pA} (V - V_A) \\ \Delta P_B &= \frac{P_B}{V_B} K_{pB} (V - V_B) \\ \Delta P_C &= \frac{P_C}{V_C} K_{pC} (V - V_C) \end{aligned} \quad (9)$$

the voltage to be applied for achieving a specified power variation ΔP is:

$$V = \frac{\Delta P + (P_A K_{pA} + P_B K_{pB} + P_C K_{pC})}{\frac{P_A}{V_A} K_{pA} + \frac{P_B}{V_B} K_{pB} + \frac{P_C}{V_C} K_{pC}} \quad (10)$$

The ST is able to impose three phase voltages with equal amplitude independently from the load, so that (10) can be simplified assuming $V_A = V_B = V_C = V_0$. The voltage variation to be applied in p.u. is now defined with the formula:

$$\frac{V}{V_0} = 1 + \frac{\Delta P}{P_A K_{pA} + P_B K_{pB} + P_C K_{pC}} \quad (11)$$

If the ST receives the request to curtail a certain amount of active power and the voltage to be applied does not exceed neither the minimum nor the maximum voltage limit, the Load Identification and Control controller applies (11).

B. ST Overload Control

The basic idea for controlling the overload conditions in the ST is to modify the voltage in the LV grid in order to

reduce the current flowing in the ST. This technique has been applied in [18] assuming the load as constant impedance and decreasing the voltage in order to reduce the load consumption. However, if the same control action is applied in a grid where the loads behave in the direction of constant power load, it will increase the current flowing in the ST. Computing the load sensitivities, the overload conditions are alleviated in real time by adapting the voltage in the grid appropriately. If the ST security current limit is exceeded in one phase, the limit controller triggers the Voltage-Based Overload Control. The On-Line Load Identification evaluates the active and reactive power sensitivities and decides to increase or decrease the voltage. Since the behavior of load active power can be different from that of reactive power, in this section the sensitivity of current with respect to voltage is evaluated for each phase taking into account both sensitivities. It is worth mentioning that the current sensitivity can also be determined by direct measurement. However, it is demonstrated in this section that the active and reactive power sensitivities are sufficient to reconstruct the sensitivity of the current.

In order to apply a balanced control action, the voltage variation to be applied to control ST overload must be the same in all phases. Consider the current and apparent power equations for one of the phases:

$$\begin{aligned} I &= S/V \\ S^2 &= P^2 + Q^2 \end{aligned} \quad (12)$$

which are linearized by taking first order partial derivatives and assuming small variations (marked with prefix Δ) around the operating point $V_0, S_0 (P_0, Q_0)$:

$$\Delta I = \Delta S/V_0 - (S_0/V_0^2)\Delta V \quad (13)$$

$$2S_0\Delta S = 2P_0\Delta P + 2Q_0\Delta Q \quad (14)$$

Substituting (3) and (14) in (13), the current variation following a voltage variation is obtained:

$$\Delta I = [(P_0/S_0)^2 K_p + (Q_0/S_0)^2 K_q - 1] (S_0/V_0^2)\Delta V \quad (15)$$

The equivalent voltage sensitivity coefficient of current K_i can be calculated as follows:

$$K_i = (\cos\varphi_0)^2 K_p + (\sin\varphi_0)^2 K_q - 1 \quad (16)$$

Thus the per unit current response to voltage changes is defined with the formula:

$$\Delta I/I_0 = K_i \Delta V/V_0 \quad (17)$$

Once the equivalent sensitivity of the apparent power is known, the voltage variation to be applied can be calculated using:

$$\begin{aligned} \text{if } I > I_{sec} \\ \frac{V}{V_0} &= 1 + \left(\frac{I_{sec} - I_{LV}}{I_{sec}} \right) / K_i \end{aligned} \quad (18)$$

where I_{sec} is the security current limit, at which the Voltage-Based Overload Control is triggered. Note that each time the above condition holds for one phase, the new V is applied to all three phases simultaneously. If the corrective voltage action calculated in one phase leads to overload another phase,

a single-phase voltage control must be applied, following the voltage sensitivity of that specific overloaded phase. However, this should be used as last resort, due to the application of intentionally unbalanced voltage and the following decrease of power quality in the grid. In this application the I_{sec} has been set equal to 95% of the ST maximum current. If K_i is positive, corresponding to a load condition in the constant impedance direction, the ST decreases the voltage to deal with the overload. If K_i is negative, the case of constant power loads, the ST increases the voltage. For conditions where $K_i = 0$, meaning a constant current load, other control strategies should be applied, i.e. Frequency-Based Overload Control with controllable resources [18].

C. Feasibility range of the voltage variation

The requested variation of the grid voltage may be not compatible with the ST design under some conditions. The ST controls the filter capacitor voltage. Due to the voltage drop on the filter inductor caused by high current with low power factor, the voltage request before the filter may be higher than the DC link voltage. In this analysis, the worst case scenario has been assumed. The current request from the load is kept constant and at the maximum current limit ($145 A_{rms}$). The ratio between the ST output peak voltage before the filter and the half of DC-link voltage (400 V) has been plotted in Fig. IV-C, varying the voltage variation request and the power factor of the net load. As can be noticed, the ratio exceeds the 1 pu value (flat gray surface in Fig. IV-C) in case of high voltage variation request (above 0.07 pu) and low power factor (below 0.9 pu, inductive). The ST parameters are listed in Table I.

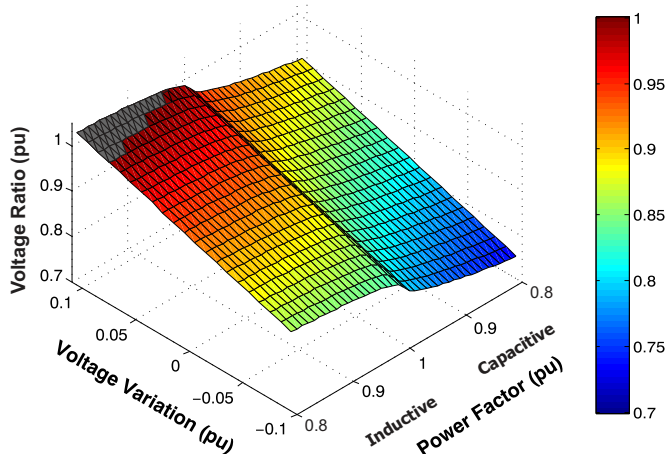


Fig. 5. Feasibility range of the voltage variation: voltage ratio between the ST output peak voltage and LV DC link voltage, depending on the voltage variation request and the net load power factor. The infeasibility region is marked with a gray area. The current is assumed constant to the maximum limit ($145 A_{rms}$).

V. EXPERIMENTAL EVALUATION OF PROPOSED CONTROLS

A. Experimental Setup

The experimental verification of ST Load Identification and associated services has been performed with the CHIL method

by means of a RTDS system in the lab setup described in Fig. V-A. The ST-fed grid, shown in Fig. 7, is implemented in RSCAD, the RTDS software. The ST control scheme described in Fig. I is implemented in dSPACE. The ST topology considered is an IGBT-based Neutral Point Clamped (NPC) converter, due to the availability of the neutral conductor connection in the DC link. The IGBT switches have the rating current of 145 A and maximum voltage equal to 1200 V, and they are implemented as equivalent model in RTDS for real time applications, as described in [27]. The switching frequency of the single IGBT is 5 kHz and Phase Disposition PWM (PD-PWM) technique has been implemented in RTDS in order to balance the DC link capacitors voltage. The modulation signals are sent by dSPACE to RTDS, where the PD-PWM is performed. The switching dead-time considered is one time step delay of the small time-step model of RTDS, in this case $1.73 \mu s$. The grid load consist of a balanced constant impedance loads, indicated with Z_L , an induction machine I_{m1} , and unbalanced constant power loads, as described in Fig. 7 and listed in Table II.

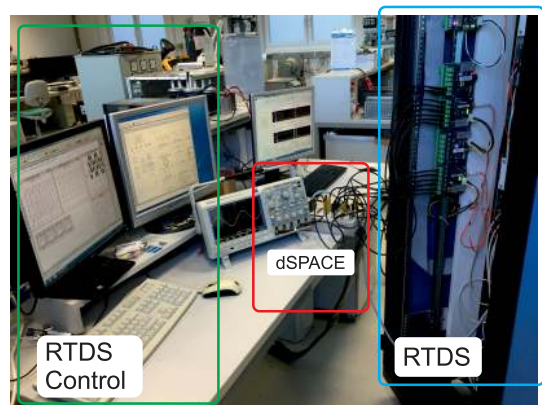


Fig. 6. Control-Hardware-In-Loop setup by means of RTDS and dSPACE realized in lab.

TABLE I
SMART TRANSFORMER DATA

ST parameter	Value	Grid Parameter	Value
S_{ST}	100 kVA	V_{rms}	230
C_{LV}	100 μF	V_{LV}^{DC}	800 V
L_{LV}	0.5 mH		

B. Soft Load Reduction

In this section, the application of the On-Line Load Identification for Soft Load Reduction purpose is shown. The ST performs load identification every 20 s (in a real application this could be every 5 – 10 minutes) and evaluates in real time the amount of voltage drop to be applied for achieving a 5% reduction of the load. A significant source of variability regarding voltage sensitivity is the varying power injection from uncontrolled DG. Thus, in order to introduce variability in the grid, the PV active power curves shown in Fig. 8 have been implemented in the two photovoltaic power plants in Fig. 7. The ramp voltage adopted in this study case to measure

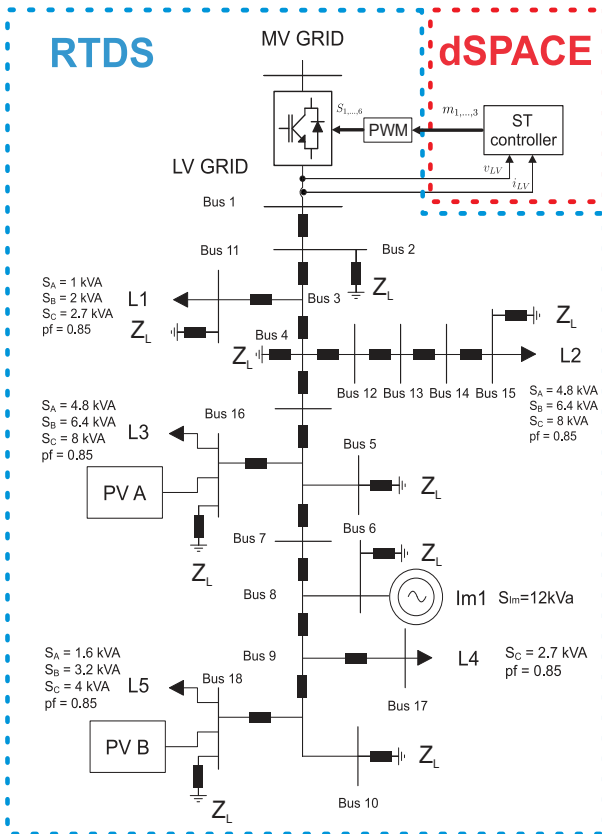


Fig. 7. ST-fed grid implemented in RSCAD and CHIL description

TABLE II
ST-FED GRID DATA

Load	Variable	Phase A	Phase B	Phase C
L_1	Apparent Power (kVA)	1	2.0	2.7
	Power Factor (pu)	0.85	0.85	0.85
L_2	Apparent Power (kVA)	4.8	6.4	8.0
	Power Factor (pu)	0.85	0.85	0.85
L_3	Apparent Power (kVA)	4.8	6.4	8.0
	Power Factor (pu)	0.85	0.85	0.85
L_4	Apparent Power (kVA)	0	0	2.7
	Power Factor (pu)	1.0	1.0	0.85
L_5	Apparent Power (kVA)	1.6	3.2	4
	Power Factor (pu)	0.85	0.85	0.85
Z_L	Apparent Power (kVA)	0.66	0.66	0.66
	Power Factor (pu)	0.9	0.9	0.9
I_{m1}	Apparent Power (kVA)	4.0	4.0	4.0
	Power Factor (pu)	0.8	0.8	0.8

load sensitivity is -0.02 p.u. over a time window of 0.5 s and the total voltage disturbance lasts 2 s. The time window as well as the magnitude of the voltage variation can vary depending on the load connected in the grid (e.g., thermostatic loads and machines with long time constant). However two constraints must be respected: *i*) a lower threshold to remove the small voltage variations caused by stochastic load; *ii*) an upper ceiling not to impact on grid power quality during the measurement. As shown in Fig. 9, at $t = 100$ s the ST receives the signal from the TSO/DSO to reduce the load by 5% for 100 s. The ST uses the active power sensitivities to voltage evaluated in the previous time interval (Fig. 9a) and applies a

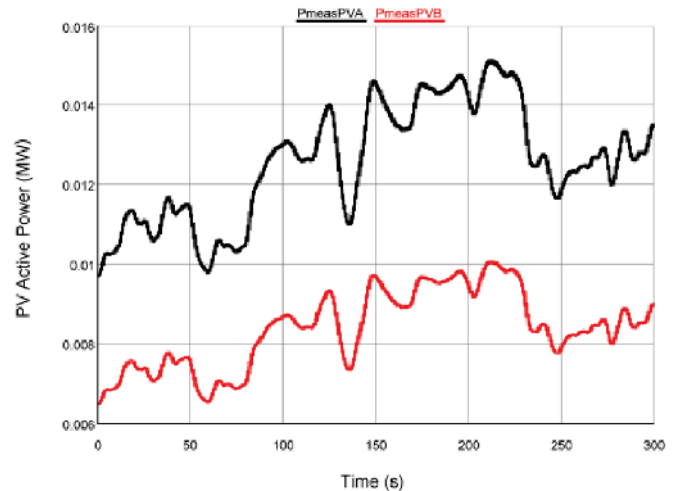


Fig. 8. Photovoltaic power plants A (black) and B (red) power curves.

reduction of 8% of the voltage (Fig. 9b). The green line in Fig. 9b is the bus 8 voltage profile, representing the lowest voltage in the grid during the load reduction. It is shown how the voltage is kept near 0.90 p.u., still acceptable considering the emergency request of load reduction by the TSO/DSO. Note that the load is less sensitive to voltage variation in this case than a constant current load ($K_P < 1$). As can be noticed from Fig. 9c,d, the average of the load shed is near 5% for the entire time window. The voltage and the load active power are restored to the nominal value when the load reduction is not needed any longer.

C. ST Overload Control

In order to demonstrate the Voltage-Based Overload Control concept the power curves described in Fig. 8 are applied to the PV plants. At $t = 100$ s the PV A is suddenly disconnected from the grid for 100 seconds (Fig. 10a), causing a current increase in the ST. If no control action is taken, the current of Phase C goes above the maximum current limit of the ST (Fig. 10b, black line), equal to $145 A_{rms}$ (Fig. 10b, red line), corresponding to $205 A_{peak}$ in sinusoidal conditions. If the Voltage-Based Overload Control is applied in this case together with the On-Line Load Identification, the voltage in all three phases is increased (Fig. 10c), decreasing the current below the maximum limit. It is worth noting that without a proper identification of the load sensitivity a voltage variation may worsen the overload condition of the ST, instead of alleviating it. In case of insufficient control range (upper or lower voltage limit), the need for energy storage elements (i.e., batteries, diesel generators) becomes essential for solving the ST overload.

VI. EXPERIMENTAL ACCURACY EVALUATION

A. Case studies

In this section the experimental verification of the On-Line Load Identification accuracy is presented. Three test cases have been analyzed: in Test Case A, the grid works in steady state

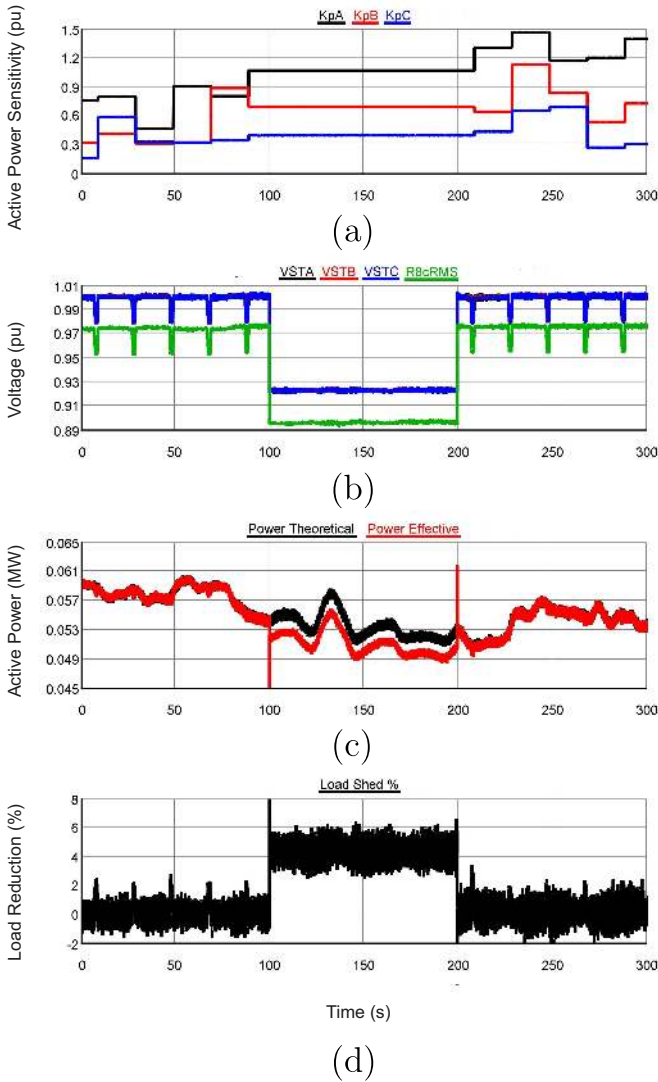


Fig. 9. Soft Load Reduction: (a) active power exponential coefficients evaluated in real time, (b) ST voltages and bus 8 voltage (green line), (c) Three-phase active power at 1 p.u. voltage (black line) and when the 5% load reduction is applied (red line), (d) load reduction in %.

and the Photovoltaic plant *A* is producing 20 kW with unity power factor. Photovoltaic plant *B* is shut down. A voltage variation of -0.05 p.u. is applied to measure the real power consumption and compare it with the estimated one calculated with the On-Line Load Identification method. In Test Case *B*, the conditions are the same as in Test Case *A*, but with a voltage variation of -0.10 p.u.. In this condition the non-linearity of the load response in case of low voltage conditions is taken in account. In Test Case *C*, the same conditions of Test Case *B* are applied with the PV *A* power production set to 0 and purely passive grid. The test cases are summarized in Table III.

In all the three test cases On-Line Load Identification is performed and subsequently the voltage variation is applied (e.g., Fig. 11, Test Case *B*). The results for the active and reactive power exponential coefficients are shown in Table IV. As expected the active power coefficients tend to decrease in the

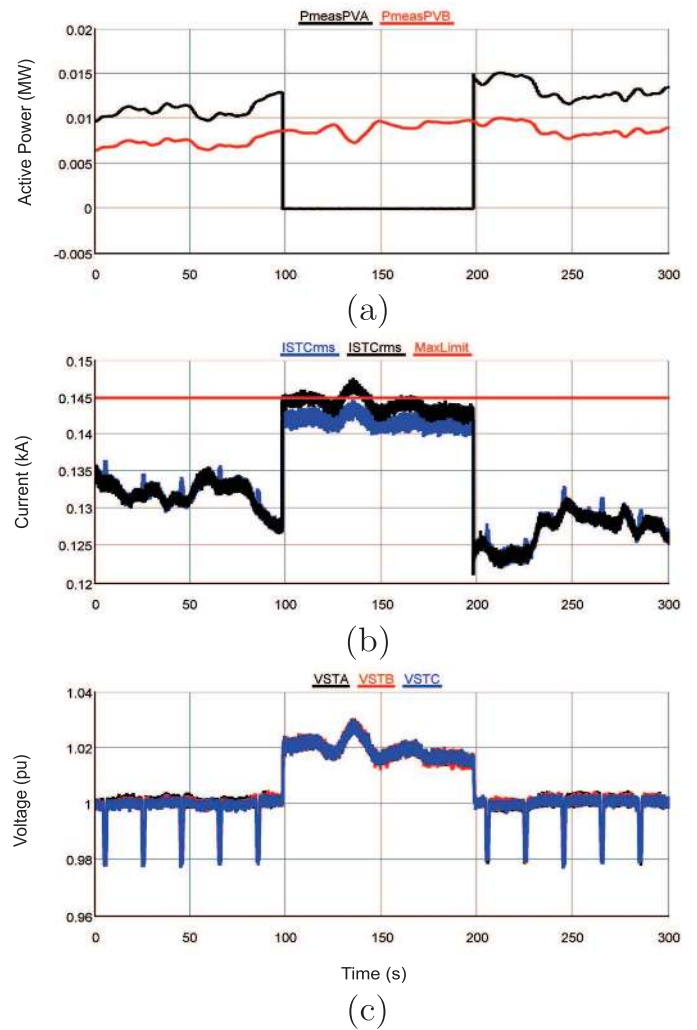


Fig. 10. Overload Control of ST: (a) PV power profiles, (b) Maximum current (red line), ST current without any applied control (black line), and ST current with Overload Control and On-Line Load Identification method (blue line), (c) ST voltages

TABLE III
ACCURACY EVALUATION TEST CASES

Test Case	Voltage Variation (p.u.)	PV <i>A</i> power (kW)
A	-0.05	20
B	-0.10	20
C	-0.10	0

absence of PV generation. This confirms what demonstrated mathematically in Section III. The reactive power coefficients remain unchanged due to the unity power factor operation of PV *A*. The accuracy of the On-Line Load Identification can be evaluated by means of the comparison between the measured powers after the voltage step and the estimated ones, obtained from the calculated active and reactive power coefficients. The relative errors of the two active and reactive powers are listed in Table V. It can be noted how the relative errors never exceed the 2% in the worst case, and when the voltage change is reduced (i.e., -0.05 p.u.) the relative errors decrease below the 1%. This is explained by the fact that the evaluation of

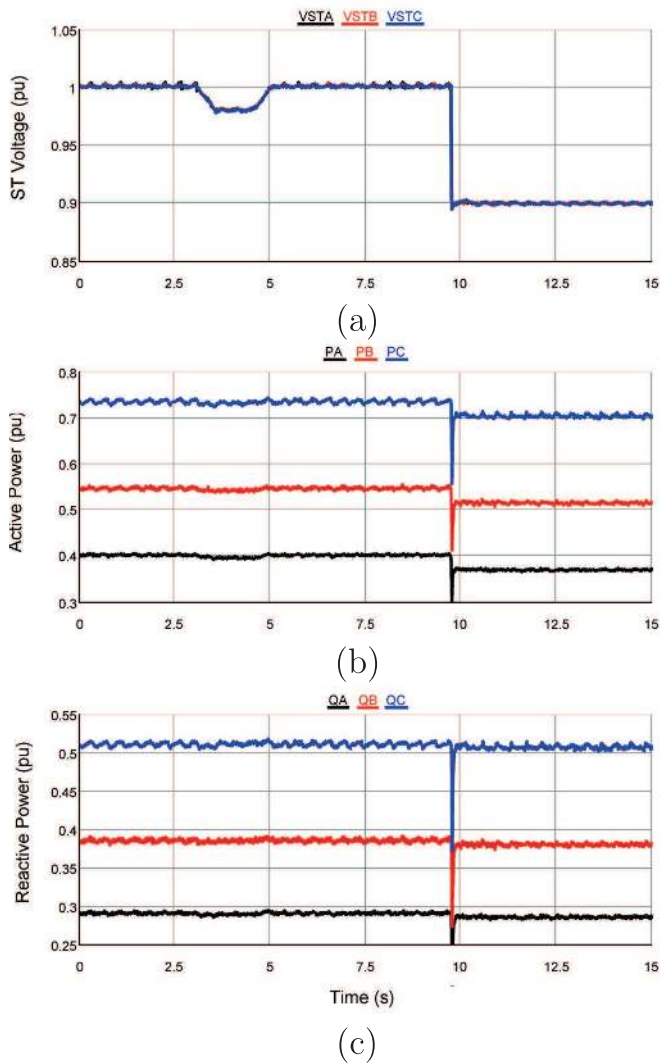


Fig. 11. On-Line Load Identification accuracy evaluation, Test Case B: (a) ST voltages, (b) ST active powers, (c) ST reactive powers.

TABLE IV
COEFFICIENTS VALUES.

Phase	Parameter	Test Case A	Test Case B	Test Case C
A	K_p	0.77	0.93	0.62
	K_q	0.35	0.34	0.29
B	K_p	0.61	0.70	0.42
	K_q	0.21	0.25	0.21
C	K_p	0.50	0.53	0.31
	K_q	0.07	0.17	0.15

the sensitivities are performed in a point (0.98 p.u.) nearer to the Test Case A voltage variation point (0.95 p.u.) than the Test Case B and C voltage variation points (0.90 p.u.).

B. Impact of DG on active power sensitivity

In Fig. 12 the measured net load voltage sensitivities in the three phases for varying DG (PV) generation are shown. Fig. 13 shows the effect (measured active power reduction) of a voltage variation of -0.05 pu applied from 100 s up to 200 s. The blue line shows the actual load reduction using

TABLE V
RELATIVE ERRORS BETWEEN THE EXPECTED POWER AND THE MEASURED ONE AFTER THE VOLTAGE VARIATION (%).

Phase	Power	Test Case A	Test Case B	Test Case C
A	P_A	0.3	1.2	1.6
	Q_A	0.8	1.8	1.7
B	P_B	0.9	0.8	1.0
	Q_B	0.6	1.3	1.4
C	P_C	0.5	1.3	0.2
	Q_C	0.2	1.8	1.0

the photovoltaic power profiles shown in Fig. 8. The black line shows the expected load reduction using the sensitivities found in Test Case C (i.e. neglecting the effect of the DG in net load sensitivity). The red line is the estimated load reduction by the On-Line Load Identification as applied in this paper. It takes into account the DG influence, using the last computed sensitivity before the load reduction, as shown in Fig. 12. The sensitivity evaluation has been performed in this case every 20 s excluding the time of voltage reduction.

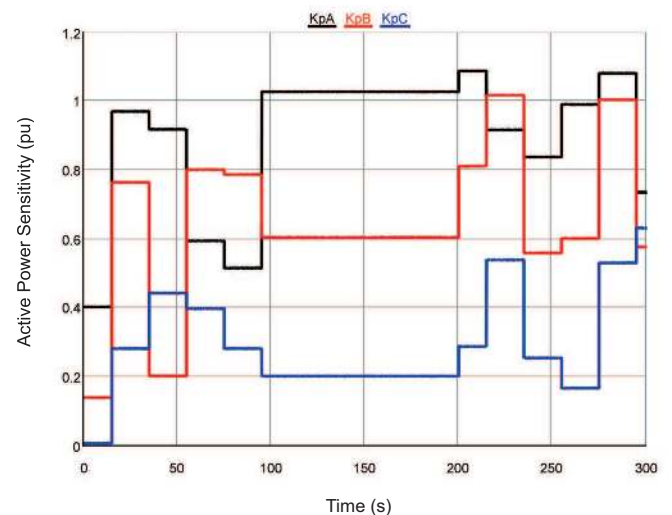


Fig. 12. Voltage dependence of net active power: sensitivity coefficients in phase A (black line), phase B (red line), and phase C (blue line).

As can be noticed, if the effect of DG is ignored an underestimation of load reduction is expected during the voltage dip (average 2.12 % reduction), which is in line with what was found in Test Case C. On the other hand, when the DG is taken into account in the net load, the expected load variation (average 2.65 %) has a better match to the average of the real load variation (2.83 %) during the voltage step. The difference with respect to the actual load reduction is due to the fact that the voltage sensitivities are calculated before the load reduction and they do not change during the transient. The actual active load reduction curve is influenced instead from the variable PV plants power production.

The results obtained in Fig. 13 confirm the main advantage that the On-Line Load sensitivity Identification has with respect to the approaches based on statistical evaluations or interpolation of long history data.

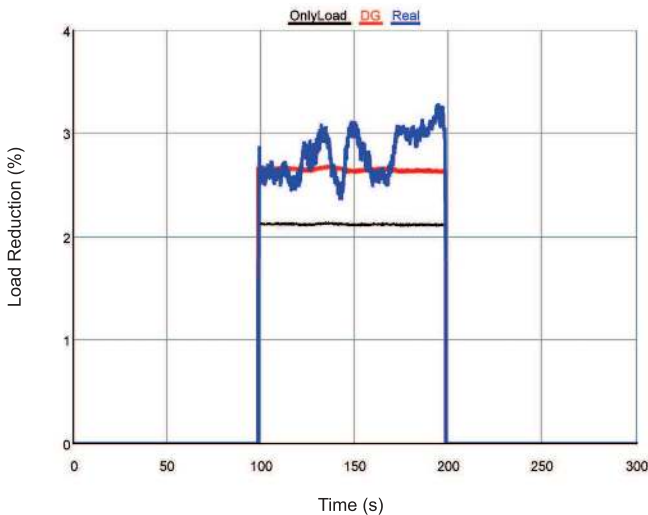


Fig. 13. Impact of DG on the voltage dependence of active power: a) load reduction estimation taking into account only passive load (black line); b) load reduction estimation using the On-Line Load Identification (red line); c) actual load reduction with varying PV injection (blue line).

VII. CONCLUSION

The Smart Transformer can provide additional services to the LV grids by controlling the output voltage, like the Soft Load Reduction control and the Voltage-Based Overload Control. The Soft Load Reduction technique enables to reduce the load active power consumption when requested by the TSO/DSO without disconnecting any load in the grid, contrary to firm load shedding. The Voltage-Based Overload Control avoids the overload conditions in the ST, acting on the consumed power of the loads. However, these two services depend on the load active and reactive power response to voltage variations. The On-Line Load Identification concept can estimate in real time the load sensitivity to voltage variations and provide more accurate control actions for these two services. The identification takes into account also the influence of the DG on the voltage sensitivities, and thus identifies the real behavior of the net aggregate load in the LV grid. In this work the load identification and control has been described and verified by means of CHIL with of RTDS. Finally the On-Line Load Identification accuracy has been evaluated and verified by means CHIL, highlighting how the DG influences the voltage sensitivities measurements.

REFERENCES

- [1] E. K. Hart, E. D. Stoutenburg, and M. Z. Jacobson, "The potential of intermittent renewables to meet electric power demand: Current methods and emerging analytical techniques," *Proceedings of the IEEE*, vol. 100, no. 2, pp. 322–334, Feb 2012.
- [2] P. Aristidou, G. Valverde, and T. Van Cutsem, "Contribution of distribution network control to voltage stability: A case study," *IEEE Transactions on Smart Grid*, vol. PP, no. 99, pp. 1–1, 2015.
- [3] G. Delille, L. Capely, D. Souque, and C. Ferrouillat, "Experimental validation of a novel approach to stabilize power system frequency by taking advantage of load voltage sensitivity," in *IEEE Eindhoven PowerTech*, June 2015, pp. 1–6.
- [4] P. J. Douglass, R. Garcia-Valle, J. stergaard, and O. C. Tudora, "Voltage-sensitive load controllers for voltage regulation and increased load factor in distribution systems," *IEEE Transactions on Smart Grid*, vol. 5, no. 5, pp. 2394–2401, Sept 2014.
- [5] M. Farrokhhabadi, C. A. Caizares, and K. Bhattacharya, "Frequency control in isolated/islanded microgrids through voltage regulation," *IEEE Transactions on Smart Grid*, vol. PP, no. 99, pp. 1–10, 2015.
- [6] W. Price, K. Wirgau, A. Murdoch, J. V. Mitsche, E. Vaahedi, and M. El-Kady, "Load modeling for power flow and transient stability computer studies," *IEEE Transactions on Power Systems*, vol. 3, no. 1, pp. 180–187, Feb 1988.
- [7] K. P. Schneider, J. Fuller, F. Tuffner, and R. Singh, "Evaluation of conservation voltage reduction (cvr) on a national level," *Pacific Northwest National Laboratory report*, 2010.
- [8] Z. Wang and J. Wang, "Review on implementation and assessment of conservation voltage reduction," *IEEE Transactions on Power Systems*, vol. 29, no. 3, pp. 1306–1315, May 2014.
- [9] I. T. F. on Load Representation for Dynamic Performance, "Load representation for dynamic performance analysis [of power systems]," *IEEE Transactions on Power Systems*, vol. 8, no. 2, pp. 472–482, May 1993.
- [10] —, "Standard load models for power flow and dynamic performance simulation," *IEEE Transactions on Power Systems*, vol. 10, no. 3, pp. 1302–1313, Aug 1995.
- [11] Z. Dong, A. Borghetti, K. Yamashita, A. Gaikwad, P. Pourbeik, and J. Milanovic, "Recommendations on measurement based and component based load modeling practice," in *CIGRE WG C4.605*, 2012.
- [12] P. Kundur, *Power System Stability and Control*. Electric Power Research Institute, 1994.
- [13] P. Regulski, D. S. Vilchis-Rodriguez, S. Djurovi?, and V. Terzija, "Estimation of composite load model parameters using an improved particle swarm optimization method," *IEEE Transactions on Power Delivery*, vol. 30, no. 2, pp. 553–560, April 2015.
- [14] L. Hajagos and B. Danai, "Laboratory measurements and models of modern loads and their effect on voltage stability studies," *IEEE Transactions on Power Systems*, vol. 13, no. 2, pp. 584–592, May 1998.
- [15] D. Han, J. Ma, R.-m. He, and Z. yang Dong, "A real application of measurement-based load modeling in large-scale power grids and its validation," *IEEE Transactions on Power Systems*, vol. 24, no. 4, pp. 1756–1764, Nov 2009.
- [16] J. Milanovic, K. Yamashita, S. Martinez Villanueva, S. Djokic, and L. Korunovic, "International industry practice on power system load modeling," *IEEE Transactions on Power Systems*, vol. 28, no. 3, pp. 3038–3046, Aug 2013.
- [17] X. She, A. Huang, and R. Burgos, "Review of solid-state transformer technologies and their application in power distribution systems," *IEEE Journal of Emerging and Selected Topics in Power Electronics*, vol. 1, no. 3, pp. 186–198, Sept 2013.
- [18] G. De Carne, G. Buticchi, M. Liserre, P. Marinakis, and C. Vournas, "Coordinated frequency and voltage overload control of smart transformers," in *IEEE PowerTech*, 2015.
- [19] G. De Carne, G. Buticchi, M. Liserre, and C. Vournas, "Frequency-based overload control of smart transformers," in *IEEE PowerTech*, 2015.
- [20] G. D. Carne, M. Liserre, and C. Vournas, "On-line load sensitivity identification in lv distribution grids," *IEEE Transactions on Power Systems*, vol. PP, no. 99, pp. 1–1, 2016.
- [21] M. Liserre, G. Buticchi, M. Andresen, G. De Carne, L. Costa, and Z. Zhiziang, "The smart transformer: Impact on the electric grid and technology challenges," *IEEE Industrial Electronics Magazine*, in press.
- [22] R. Pena-Alzola, G. Gohil, L. Mathe, M. Liserre, and F. Blaabjerg, "Review of modular power converters solutions for smart transformer in distribution system," in *IEEE Energy Conversion Congress and Exposition (ECCE)*, Sept 2013, pp. 380–387.
- [23] G. Buticchi, G. D. Carne, D. Barater, Z. Zou, and M. Liserre, "Analysis of the frequency-based control of a master/slave micro-grid," *IET Renewable Power Generation*, June 2016. [Online]. Available: <http://digital-library.theiet.org/content/journals/10.1049/iet-rpg.2016.0167>
- [24] T. Van Cutsem and C. Vournas, *Voltage Stability of Electric Power Systems*. Kluwer Academic Publishers, 1998.
- [25] C. W. Taylor, "Concepts of undervoltage load shedding for voltage stability," *IEEE Transactions on Power Delivery*, vol. 7, no. 2, pp. 480–488, Apr 1992.
- [26] I. Industrial and C. P. S. Committee, "Report on reliability survey of industrial plants, part ii: Cost of power outages, plant restart time, critical service loss duration time, and type of loads lost versus time of power outages," *IEEE Transactions on Industry Applications*, vol. IA-10, no. 2, pp. 236–241, March 1974.
- [27] *VSC Valves and Breakers, RTDS manual*.



Giovanni De Carne Giovanni De Carne (S'14) was born in Noci, Bari (Italy) in 1988. He received the bachelor and master degrees in Electrical Engineering from Politecnico di Bari (Italy) in 2011 and 2013, respectively. In 2013, he started working on his Ph.D. studies at the Chair of Power Electronics at University of Kiel, Germany. He is currently working on his PhD "Analysis of ST features for electric distribution grid" within the ERC Grant project "Highly Reliable And Efficient smart Transformer (HEART)".



Giampaolo Buticchi Giampaolo Buticchi (S'10-M'13) was born in Parma, Italy, in 1985. He received the Masters degree in Electronic Engineering in 2009 and the Ph.D degree in Information Technologies in 2013 from the University of Parma, Italy. He is now working as a postdoctoral research associate at the University of Kiel, Germany. His research area is focused on power electronics for renewable energy systems, smart transformer fed micro-grids and reliability in power electronics.



Marco Liserre Marco Liserre, (S'00-M'02-SM'07-F13) is Full Professor and Head of the Chair of Power Electronics at the University of Kiel (Germany). He has published over 200 technical papers and a book, for them he is listed in ISI Thomson report The worlds most influential scientific minds. He has been awarded with an European ERC Consolidator Grant, one of the most prestigious in Europe, to make research about Smart Transformer. He did serve IAS, PELS, PES and IES in various capacities such as reviewer, associate editor, editor, conference chairman or track chairman and Vice-President. He has received several IEEE Awards.



Costas Vournas Constantine (Costas) Vournas (S'77-M'87-SM'95-F'05) received the Diploma of Electrical and Mechanical Engineering from the National Technical University of Athens (NTUA) in 1975, the M.Sc in Electrical Engineering from the University of Saskatchewan, Saskatoon, Canada in 1978, and the NTUA Doctor of Engineering degree in 1986. He is currently Professor in the Electrical Energy Systems Laboratory of the School of Electrical and Computer Engineering of NTUA. He has co-authored the book Voltage Stability of Electric Power Systems. His research interests are in the area of power system dynamics, stability and control and include voltage stability and security analysis, wind generator integration in power systems, novel control applications in the distribution and transmission grid, as well as the effect of deregulation on power system operation and control.